DEUTSCHES ELEKTRONEN-SYNCHROTRON DESY
DESY SR 89-05
September 1989

Surface Temperature and Slope Errors on Plane Mirrors Exposed to High Power Synchrotron Radiation

W. Jark, S. Mourikis
Fritz-Haber-Institut der Max-Planck-Gesellschaft, Berlin
S. Joksch, V. Saile
Hamburger Synchrotronstrahlungslabor HASYLAB at DESY, Hamburg

ISSN 0723-7979

NOTKESTRASSE 85 · 2 HAMBURG 52

To be sure that your preprints are promptly included in the HIGH ENERGY PHYSICS INDEX , send them to the following address (if possible by air mail) :

DESY
Bibliothek
Notkestrasse 85
2 Hamburg 52
Germany

DESY SR 89-05
September 1989

ISSN 0723-7979

Surface Temperature and Slope Errors on Plane Mirrors Exposed to High Power Synchrotron Radiation

Werner Jark (*) and Spiridon Mourikis (**)
Fritz-Haber-Institut der Max-Planck-Gesellschaft,
Faradayweg 4-6, D-1000 Berlin 33, Germany

(*) now with Sincrotrone Trieste, Padriciano 99, I-34 012 Trieste, Italy
(**) now with Universität Dortmund, Experimentalphysik I, Postfach 500 500, D-4600 Dortmund 50, Germany

Stefan Joksch and Volker Saile
Hamburger Synchrotronstrahlungslabor HASYLAB at
Deutsches Elektronen-Synchrotron DESY, Notkestr. 85,
D-2000 Hamburg 52, Germany

Abstract

The temperature at the surface and the distortion of plane mirrors made from different materials have been investigated with incident surface power densities of the order of 0.4 W/mm^2 and total powers of up to 170 W. While the surface temperature could be significantly lowered with increasing cooling water flow rate, the temperature gradients and the deformation of the surface were found to be too much superior to all other samples. Contrary to the theoretical expectations the surface distortion was found to depend not only on the figure of merit for thermal distortions. This is interpreted by taking into account the penetration depth of the radiation emitted by the hard x-ray wiggler (HARWI) in 5.3 GeV storage ring DORIS.

This project was supported by the Bundesministerium für Forschung und Technologie with contract No. 05 265 KO IO.

To be published in Nucl. Instrum. and Meth. in Phys. Res, Volume A, Proceedings of 6th National Conf. on Synchrotron Radiation Instrumentation, 7-10 August, 1989, Berkeley CA, USA.

I. Introduction

Intense synchrotron radiation emitted from state-of-the-art wiggler and undulator beamlines at the various synchrotron radiation laboratories is able to distort the optical surfaces significantly or even to destroy the optical components exposed to the "white beam" [1,2]. The present paper deals with deformations of plane mirrors due to heat loads which are well below the destruction threshold. The only parameter that affects the performance of these mirrors is the slope error of the surface.

In order to find suitable materials and cooling configurations we systematically investigated the deformation of several different standard mirror materials in our exposure station [3,4] under worst case conditions: A high power beam being incident almost normal to the surface. We present results that have been obtained almost exclusively with radiation from the hard x-ray wiggler W2 [5] in the DORIS storage ring operated at an electron energy of 5.3 GeV. Results obtained for the heat transfer into the cooling channels, the temperature gradient in the test mirror and the bending of the surface will be compared to theoretical expectations. The comparison demonstrated that not only the total power or power density but also the spectral distribution of the incident radiation has to be taken into account especially for high energy storage rings.

II. Experimental conditions

1.) Instrumentation

a.) sample holder

A sideview of the components in our test station [3] as used in the present study is shown schematically in figure 1. The radiation is being incident almost normal to the surface of the mirror which was placed at about 28 m from the wiggler source. The sample is in the centre of a vacuum chamber that is separated from the vacuum system of the beamline by a 1 mm Be window. The detectors are mounted outside looking through appropriate viewports (infrared (IF) transparent window and high quality plane parallel plate).

All the samples were "glued" with an InGaSn eutectic to a directly water cooled copper plate. This sample holder has a closed loop water channel with a diameter of 5 mm and 10 mm distance between the centers of the in- and outlet. The channels are oriented symmetrically to the incident beam with the

smallest distance to the copper-mirror interface of only 1 mm. The orientations of the beam and the interferometer with respect to the sample holder geometry are drawn in figure 2 which is a view normal to the mirror surface. Between the 2 cooling channels a thermocouple was mounted in the centre of the illuminated area at 1 mm distance from the interface (see figure 1). Thus it is close to the back surface of the sample and also close to the cooling channels surface. Neglecting both the temperature gradient in the copper holder and over the thin "glue" layer the rading from this thermocouple is a good approximation for the temperatures at the two points mentioned. Additional thermocouples were mounted to the water inlet and outlet pipes outside the vacuum chamber. Another one was connected to the surface of the sample outside the illuminated area but still in the field of view of the IR camera. All thermocouples were of the Chromel/Alumel type and provided the temperature with an accuracy of 0.5 C. The water flow could be regulated by a flowmeter (error approximately 10 % of the smallest applied flow rate) in the inlet tube. Thus we have been able to monitor the following quantities simultaneously:

water velocity V
water inlet temperature T_{in}
water outlet temperature T_{out}
temperature at the back of the sample T_b
temperature at the side of the sample T_s

b.) Samples

Results for the following materials will be presented here: Cu, Mo, Ge, Si and a SiC CVD coating (420 µm) on a high purity graphite substrate [6] in the following denoted SiC/C. In the course of the experiments the latter sample was coated with 30 nm Au for a coating test. For both Cu and Si we tested samples with different thickness, 3 mm and 9 mm for Cu and 2 mm and 6 mm for Si crystals, respectively. The other samples had thicknesses of 11 mm for Mo, 4,8 mm for a Ge crystal and 10 mm for the SiC/C samples. The Cu and Mo mirrors were of circular shape with diameter 50 mm, while the others were rectangular with lengths 40 mm x 60 mm (Si) and 35 mm x 40 mm (SiC), respectively. The Ge crystal had approximate dimensions of 21 mm x 57 mm. For Ge and Si we also measured their bulk deformation in an independent investigation in a high power beam in a double crystal monochromator [7].

c.) Infrared camera

The temperature in the center of the illuminated area was determined with the attached IR-camera (Inframetrics 522), which is sensitive in the wave-

length range λ = 8 µm to 12 µm. It has a spatial resolution of 4 mrad, corresponding to an ellipse with 2 mm x 3 mm at the sample surface for our geometry.

Besides of uncoated SiC all other samples exhibited strange behaviour in the IR regime which makes the data reduction rather difficult. For instance the IR-absorption of Ge and consequently its emissivity is strongly temperature dependent [8]. In order to avoid any ambiguitis and calibration procedures for all the different samples we coated 5 mm wide stripes on the samples with graphite (see figure 2). In a systematic investigation we tested stripes with various widths on different substrates by heating the sample from the back in the range 20° C up to 120° C. As long as the stripe width exceeded 5 mm which is more than twice of the IR-camera resolution all calibration curves were identical within the experimental error of about 2° C. This calibration curve was found to be in very good agreement with the one provided for the IR camera for a sample emissivity of 0.85. During the experiments the calibration could always be crosschecked with the thermocouple touching the side of the crystal in the field of view of the IR camera.

d.) Interferometer

The surface deformation was measured with a Michelson interferometer oriented normal to the inspected surface. It provided a field of view with diameter 22 mm (figure 2). During the exposures the interferogramms were recorded with a videocamera. Videocopies made afterwards from the playback picture allowed to measure wavefront distortions with an accuracy of 1/10 of the wavelength of the He-Ne laser (λ = 632.8 nm).

Under steady state conditions all the power being absorbed in the test mirror will be transfered to the cooling water since radiation losses are negligible at the observed temperatures of T < 80° C. Hence the temperature difference in the water circuit and the water flow rate enable us to calculate the incident power with an error of less than 10 %. We are therefore able to determine the incident power P, the temperature gradient ΔT_s across the surface of the mirror and the temperature gradient ΔT normal to the mirror surface. All samples were measured with DORIS running at an electron energy of 5.3 GeV besides the SiC/C mirror which was measured at the reduced energy of 3.7 GeV.

2.) Incident beam characteristics

With the water flow rare in the sample holder fixed the repeatability and the detection limit for the incident power are of the order of 1 W, which allowed us to scan the profile of the incident power at 15.5 m from the source. Figure 3 presents data for the vertical profile measured by scanning an aperture with dimensions 1 mm (vertical) x 20 mm (horizontal) at this position across the incident beam. These curves could be well fitted by gaussians. A calculation [9] assuming a point source and taking into account the absorption in the beamline filters (0.4 mm C and 3 mm Be) yields a standard deviation σ = 0.78 mm, which is just 1/3 of the measured result σ = 2.34 mm. The corresponding numbers for 3.7 GeV are σ (measured) = 1.30 mm and σ (point source) = 0.96, with a ratio of 3/4. The results can be understood taking into account the electron optics in the straight section of the wiggler W2. In particular, the vertical divergence of the electron beam during 5.3 GeV high energy physics operation is larger than that of the synchrotron radiation beam. This results in a significantly increased beam height as compared to a point source with negligible electron divergence. With the measured beam profiles we obtain power densities at the sample of approximately 0.46 W/mm^2 and 0.41 Wmm^2 for the standard conditions 5.3 GeV with beamcurrent I = 30 mA and 3.7 GeV with I = 85 mA, respectively. The calculated spectral power distribution in the orbit plane and displaced 0.1 mrad above is displayed in figure 4.

In the present investigation we varied the incident power by measuring at different electron beam currents as well as by closing the aperture in the beamline. In order to test the cooling efficiency we also changed the water flow rate systematically. The dependence of the measured data on thickness was investigated with copper mirrors and with Si crystals of different thickness.

III. Results

Table 1 presents some of the results for comparable incident power. The beam dimensions at the sample position were defined by the slit system to 37 mm in the horizontal and 12 mm in the vertical direction, respectively. For E = 5.3 GeV the full-width-of-half-maximum (FWHM) of the power distribution is 9.9 mm ($2.35 \cdot \sigma$ = 4.2 mm) which is almost the vertical window dimension. The corresponding number for 3.7 GeV ist FWHM = 4.2 mm.

The curvature of the mirror under thermal load was determined with the Michelson interferometer along the direction perpendicular to the orbit plane. In the pictures the distortion of the fringes was measured at a position close to the graphite stripe at 7 points equally spaced over the field of view.

After correcting for the distortion of the unexposed mirror the results can be drawn as height profiles which are presented in figure 5. In all cases we found a bending of the whole mirror rather than a local bump on the surface. The slope errors θ presented in table 1 correspond to the maximum slope of the profiles shown in figure 5. They are accurate to within 10 µrad. Due to the limited field of view of the interferometer we cannot say whether the slope is somewhat larger outside this field.

IV. Discussion

1.) Temperature gradients

The average temperature of the sample can be significantly reduced by increasing the water flow rate, as demonstrated in Table 1. However, this does not affect the temperature gradient between surface and back side of the tested mirror. Neither does it change the lateral gradient. This was also examined by rocking curve measurements on germanium crystals exposed to intense synchrotron radiation [7].

Since the beamsize is much lager than the mirror thickness, the gradient could be approximated by an onedimensional heat flow model which leads to:

$$\Delta T_p = P' \cdot d/K \qquad (1)$$

where P'is the surface power density. d and K are the thickness of the mirror and its thermal conductivity, which is presented in Table 2.

If we assume that the power is homogeneously distributed over the beam we obtain the gradients ΔT_p presented in table 1. These results are indeed always close to the measured values, although the accuracy for ΔT is rather limited for the thin mirrors. Only the 6 mm thick Si sample shows a significantly lower temperature gradient than calculated.

The radius of curvature R due to thermal bending of the mirrors is given by [10]:

$$R = d/a \cdot \Delta T \qquad (2)$$

Here a is the thermal expansion coefficient. With our definition of the slope error θ the following relationship holds:

$$2\theta = L/R$$

where L is the width of the illuminated area. Consequently we calculate the temperature gradient responsible for the bending of the mirror as:

$$\Delta T_b = 2 \cdot d \cdot \Theta / a \cdot L \qquad (3)$$

The results of these calculations, where we set L = FWHM of the power distribution at the surface are also presented in table 1 and denoted by ΔT_b. These temperature gradients are almost 50 % larger than those measured. This discrepancy is due to the fact that the slope error results from a superposition of the bending of the whole sample and the local distortion due to the bump.

2.) Surface distortion

The comparison of the height profiles drawn in figure 5 for different water flow rates in one mirror shows that the surface distortion is not affected by the cooling efficiency. Neither does it in the case of Cu obviously depend on the sample thickness. Theoretically as shown in equation (2) the surface distortion is expected to be proportional to the figure of merit - the ratio of thermal expansion coefficient to thermal conductivity (see table 1). In table 1 we compare the slope errors normalized for 100 W incident power to the figure of merit and found a good agreement with the exception of Si and SiC/C. For both materials the slope errors are much smaller than expected from considering the heat load on the surface only. The reason for the discrepancy is the small absorption coefficient, i.e. the large penetration depth of the radiation in these low Z materials. For the experiments described here the spectral distribution of the radiation as sketched in figure 4 has to be taken into account.

Taking the theoretical spectral distribution and the absorption coefficients of the elements tested we can calculate the power that transmits through a depth of 1 mm [9]: Ge (13 %), Cu (10 %), Mo (3 %), Si (64 %) and C(SiC/C at 3.7 GeV: 94 %).

In the metals and in Ge 85 % of the power is absorbed in the first millimeter so that our simplifying assumptions for the calculations are justified. On the other hand for Si and especially for the SiC/C mirror the absorption takes place over all of the sample thickness. Furthermore, a significant amount of the radiation is transmitted through the whole sample and absorbed in the copper holder. Thus the real temperature gradient will be smaller than calculated

under our worst case assumptions. The large penetration depth of hard x-rays in Si and SiC combined with the excellent figure of merit of these low Z materials are the basis of their superior properties as optical components in intense x-ray beams.

3.) Cooling efficiency

With the incident power P and the average temperature difference between the cooling water and the substrate holder ΔT_c we are able to calculate an average value for the heat transfer coefficient $P/\Delta T_c$ into the water. This value should be independent of the sample. A useful equation for its calculation is given by Ulc and Sharma [11] (it is consistent with an equation given by Avery [12]):

$$T[W/^oC] = 0.01\ A[mm^2] \cdot (0.583 + 0.0079\ T_H[^oC]) V^{0.8}[m/s] / D^{0.2}[mm] \qquad (4)$$

with T_H being the water temperature, V the water velocity., D the channel diameter and A the effective cooling channel surface. If we take for the effective cooling surface in equation [4] the total perimeter of the cooling channels with only the illuminated length of 37 mm this leads to the line denoted by "calculation" in figure 6. Since the total cooling channel surface is just twice the value given above, the coefficient can be at most twice as large. A few measured examples are also drawn in figure 6. For all samples the transfer is almost twice as efficient as expected, which could mean that a significant amount of power flow takes place to the side parallel to the surface spreading the power over all of the holder, so that the whole water loop contributes to the cooling. Certainly, also in this case we have to take into account the transmission of hard x-rays through the low Z materials. With the power being absorbed closer to the cooling channels, less area of the cooling channels outside of the illuminated area will contribute to the heat transfer thus reducing the total heat transfer coefficient. This is indeed observed for Si.

4.) Finite element analysis

A comparison of our results with finite element analysis is currently underway [13]. First results for Ge are in close agreement with the experiments: temperatures are well reproduced, the slope is 2/3 of the measured value.

V. Conclusion

We have described heat load experiments performed under worst case conditions (almost normal incidence) on plane mirrors of different materials. The surface temperature could be reduced with increasing water flow. Useful estimates for the heat transfer coefficients into the cooling water were calculated assuming a turbulent flow of the cooling liquid. In all cases the cooling efficiency neither affected the temperature gradient into the test mirror nor the bending of the mirror. If the power is absorbed in a negligibly thin surface layer some simple equations were found to give results in good agreement with the measurements for this temperature gradient as well as for a lower limit for the bending. In this case and under otherwise similar conditions the observed bending is proportional to the figure of merit for surface distortion. Si and SiC/C are found to be much superior to the other materials. Not only that the figure of merit for these materials is high but also the large penetration depth of hard x-rays results in a dissipation of the incident power in a large volume. Therefore the real figure of merit is even higher than expected from thermal expansion and conductivity only.

We demonstrated in particular in this paper the importance of considering the spectral power distribution of the incident radiation for the heat load problems, especially for low Z materials and insertion devices emitting high photon energies.

References:

[1] A.A. MacDowell, J.B. West and T. Koide, Nucl. Instrum. Meth. A246, 219 (1986)

[2] P.Z. Takacs, J. Melendez and J. Colbert, Nucl.Instrum. Meth. A246, 207 (1986)

[3] S. Mourikis, E.E. Koch and V. Saile, Nucl. Instrum. Meth. A267, 218 (1988)

[4] S. Mourikis, W. Jark, E.E. Koch and V. Saile, Rev. Sci. Instrum. 60(7), 1474 (1989)

[5] U. Hahn, W. Graeff, E.W. Weiner and L. Bitter, Proc. of Conf. on "Vacuum Design of Advanced and Compact Synchrotron Radiation Light Sources", May 16-18, 1988, Upton, NY, ed. by American Vacuum Society

[6] S. Sato, A. Iijima, S. Takeda, M. Yanagihara, T. Miyahara, A. Yagishita, T. Koide and H. Maezawa, Rev. Sci. Instrum. 60(7), 1479 (1989)

[7] St. Joksch, D. Degenhardt, R. Frahm, G. Meyer and W. Jark, Nucl. Instrum. Meth., submitted

[8] Handbook of Optics, ed. W.G. Driscoll and W. Vaughan, McGraw Hill, NY, (1978), page 7-29

[9] Calculated with the HASYLAB-program package SPECTRA (W. Graeff and T. Wroblewski)

[10] J. Kalus, G. Gobert and E. Schedler, J. Phys. E 6, 488 (1973)

[11] S. Ulc and S. Sharma, Nucl. Instrum. Meth. A246, 423 (1986)

[12] R.T. Avery, Nucl. Instrum. Meth. 222, 146 (1984)

[13] W. Jark, C. Lenardi and St. Joksch, to be published

Table 1: Experimental results for the mirrors obtained at comparable incident powers.

Numbers in front of the element abbreviations indicate the sample thickness. V is the cooling water velocity in the sample holder and P is the incident power. While T_S and T_b are the temperatures measured with thermocouples at the side and at the back of the mirror, T_{max} is the temperature measured with the IR camera in the center of the illuminated area. The bend angle Θ was derived as half of the maximum slope change at the mirror surface in the field of view of the interferometer. ΔT is the difference T_{max} - T_b. ΔT_ρ is the temperature difference calculated assuming onedimensional heat flow in the mirror according to equation (1). ΔT_b is the temperature difference that is needed in order to describe the measured bend angle Θ with equation (3). $\overline{\Theta}$ is the average of the bend angles normalized to 100 W incident power. a/K is the figure of merit from table 2.

(*) could not be determined due to the unexposed mirror being too much distorted.

(**) not given, because the width of the power distribution is significantly different to those for all other examples.

Table 2: Thermal properties for the investigated samples:

Table 2:

Substrate (element)	Thermal conductivity K [W/(cm*K)]	Thermal expansion a * 10^{-6} [1/°K]	Figure of merit a/K *10^{-6} [cm/W]
Ge	0.6	6.0	10.0
Cu	4.0	16.0	4.0
Mo	1.38	5.0	3.62
Si	1.5	2.6	1.7
C (SiC/C)[6]	0.8-2.0	4.4	2.2-5.5

TABLE 1:

sample	V [m/s]	P [W]	T_S [°C]	T_b [°C]	T_{max} [°C]	Θ [µrad]	Θ ["]	ΔT [°C]	ΔT_ρ [°C]	ΔT_b [°C]	$\overline{\Theta}$ [µrad]	a/K *10^{-6} [cm/W]	K/a [rad W/cm]
4.8 mm Ge	0.25	119	64.3	51.7	79.2	250	52	27.5	22.4	35.3	215	10.0	21.5
	0.66	109	52.0	37.5	61.0	240	50	23.5	20.6	33.9			
9 mm Cu	0.25	101	44.7	43.3	49.3	80	17	6.0	5.4	7.9	85	4.0	21
	0.66	94	34.7	31.5	37.3	85	18	5.8	5.0	8.5			
3 mm Cu	0.25	106	44.5	45.5	50.0	85	18	4.5	1.9	2.8	85	4.0	21
	0.66	98	35.7	34.7	41.0	88	18	6.3	1.8	2.9			
11 mm Mo	0.25	129	53.7	50.0	69.5	83	17	19.5	24.2	32.2	70	3.6	19
	0.44	120	46.8	39.7	60.8	90	18	21.1	22.5	35.0			
2 mm Si	0.25	129	49.0	54.6	59.1			4.5	4.1	(*)			
6 mm Si	0.25	113	46.3	49.0	55.4	33	7	6.4	10.7	11.7	27	1.7	16
	0.66	130	37.0	38.3	46.0	33	7	7.7	12.2	11.7			
10 mm C+ 420 µm SiC	0.25	85	63.7	40.7	66.1	25	5	25.4	(**)	25.1	29	2.2-5.5	13-5

Figure captions:

1). Sideview of the configuration used for this investigation (angle of incidence for the synchrotron radiation 28°): M = test mirror, MI = Michelson interferometer, IR = Infrared camera, H = cooled mirror holder (full dots represent the water channels), SR = incident synchrotron radiation, T = thermocouples.

2.) Top view of the experimental arrangement at the sample holder of dimensions 73 mm x 50 mm: H_2O = water channels, C = carbon stripe position at sample, Cu = Cu-plate, MI = field of view (diameter 22 mm) of the Michelson interferometer, Th = thermocouple touching the side of the test mirror. The shaded rectangle defines the illuminated area.

3.) Measured vertical power distribution at the wiggler W2 station for an electron beam energy of 5.3 GeV (beam current 30 mA) with an aperture of 1 mm x 20 mm positioned 15.5 m from the source. The solid curve corresponds to a gaussian with a sigma of σ = 2.34 mm.

4.) Spectral power density calculated for a point source at the wiggler W2 station and for an aperture of 1 mm x 20 mm positioned 28 m from the source. Curve a is for the aperture in the orbit plane while curve b is for a 3 mm displacement vertical to this plane. The absorption in 0.4 mm C and 3 mm Be filters which are installed in the beam line has been taken into account.

5.) Height profiles in units of fringe separation (1 fringe = 0.316 nm) versus position. For each sample (see Table 1) the upper curve corresponds to a water velocity of 0.25 m/s while the lower one was measured for 0.66 m/s (0.44 m/s in the case of Mo). The thickness is indicated at the left. The errors are of the order of 0.1 fringes.

6.) Heat transfer coefficient into the water versus water velocity V: comparison between the measured values (1 = Cu 9 mm, 2 = Mo, 3 = Si 6 mm, 4 = Ge) and the calculation for the present geometry (see text). For clarity no error bars are drawn, they are about 10% for small and 5% for large velocities.

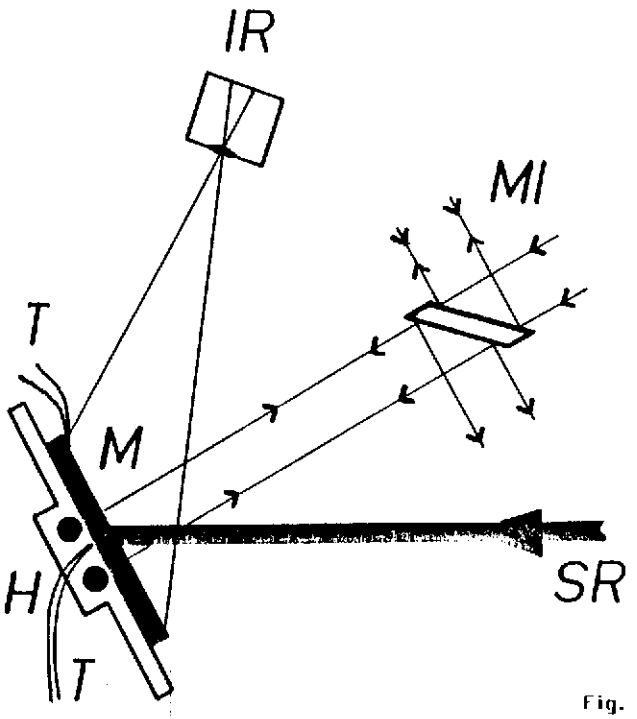

Fig. 1

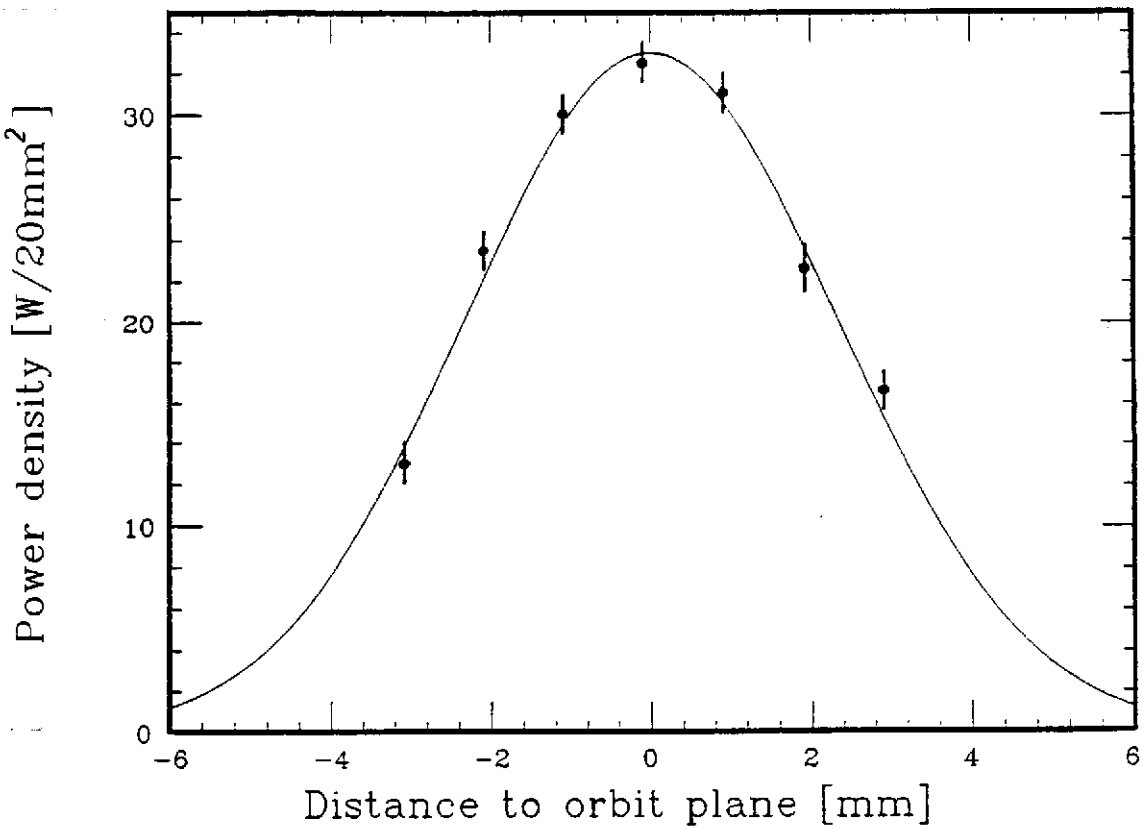
Vertical power profile
Power density [W/20mm^2]
30
20
10
0
−6
−4
−2
0
2
4
6
Distance to orbit plane [mm]

Fig. 3

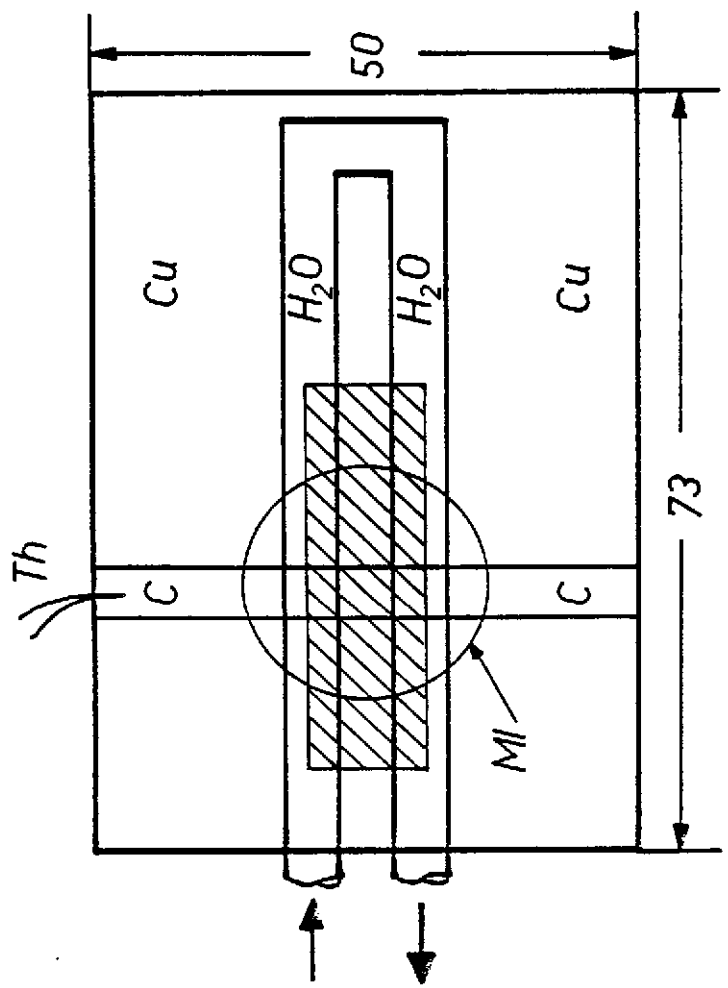
50
Cu
H_2O
H_2O
Cu
73
Th
C
C
MII

Fig. 2

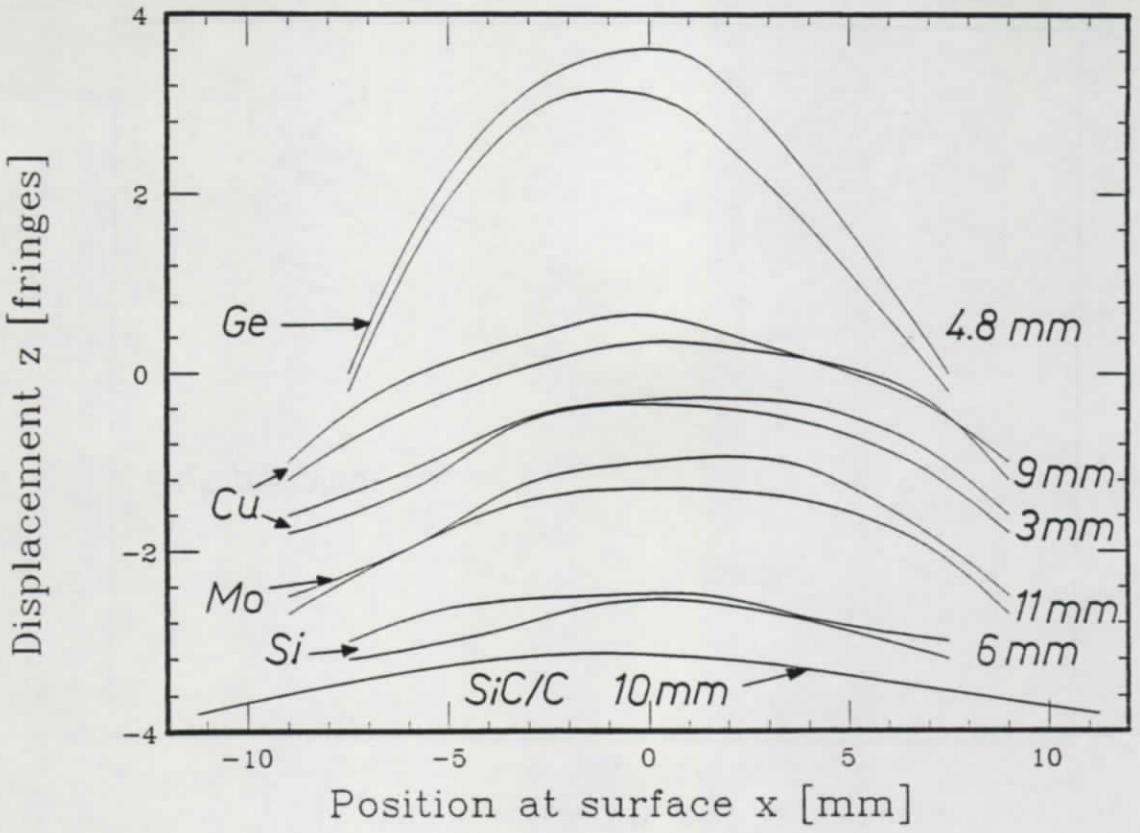
Height profile across surface
Displacement z [fringes]
Position at surface x [mm]
Ge
Cu
Mo
Si
SiC/C
4.8 mm
9mm
3mm
11mm
6mm
10mm
4
2
0
-2
-4
-10
-5
0
5
10

Fig. 3

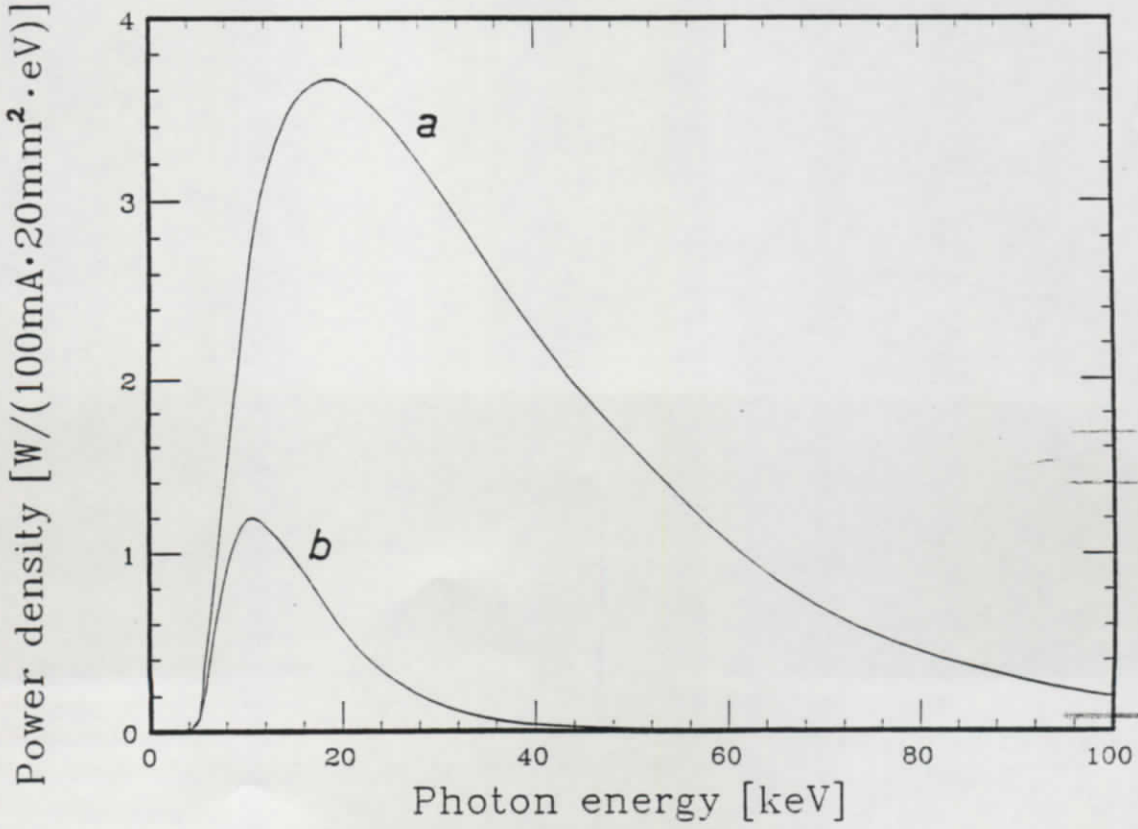
Spectral power distribution
Power density [W/(100mA·20mm²·eV)]
Photon energy [keV]
a
b
4
3
2
1
0
0
20
40
60
80
100

Fig. 4

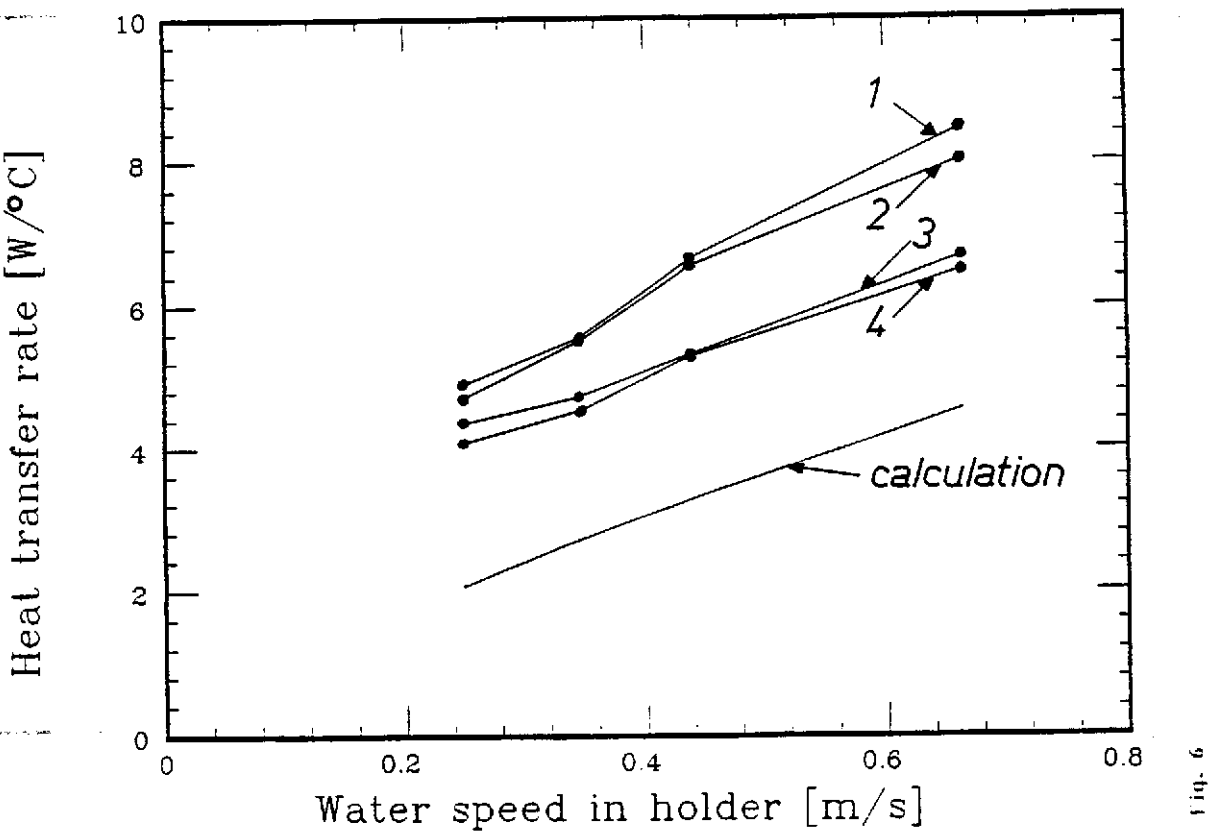
Heat transfer into cooling water
Heat transfer rate [W/°C]
10
8
6
4
2
0
0
0.2
0.4
0.6
0.8
Water speed in holder [m/s]
1
2
3
4
calculation

Fig. 6